AD A045546

(1)

RADC-TR-77-202
Technical Report
June 1977

IR ATMOSPHERIC MEASUREMENTS

AVCO Everett Research Laboratory, Inc.

Sponsored by
Defense Advanced Research Projects Agency (DoD)
ARPA Order No. 2646

ROME AIR DEVELOPMENT CENTER
Air Force Systems Command
Griffiss Air Force Base, New York 13441

This report has been reviewed by the RADC Information Office (OI) and is releasable to the National Technical Information Service (NTIS). At NTIS it will be releasable to the general public, including foreign nations.

This report has been reviewed and is approved for publication.

APPROVED: James W Cusack

JAMES W. CUSACK
Project Engineer

MISSION
of
Rome Air Development Center

RADC plans and conducts research, exploratory and advanced development programs in command, control, and communications (C^3) activities, and in the C^3 areas of [illegible]ation sciences and intelligence. The principal techni[illegible]sion areas are communications, electromagnetic gui[illegible]nd control, surveillance of ground and aerospace objects, intelligence data collection and handling, information system technology, ionospheric propagation, solid state sciences, microwave physics and electronic reliability, maintainability and compatibility.

AMERICAN REVOLUTION BICENTENNIAL 1776-1976

IR ATMOSPHERIC MEASUREMENTS

H. P. Kent
P. F. Kellen

Contractor: AVCO Everett Research Laboratory, Inc.
Contract Number: F30602-75-C-0235
Effective Date of Contract: 29 June 1975
Contract Expiration Date: 30 June 1977
Short Title of Work: IR Atmospheric Measurements
Program Code Number: 5E20
Period of Work Covered: Jun 75 - Feb 76

Principal Investigators: H. P. Kent and P. F. Kellen
Phone: 617 389-3000 Ext. 282/398
Project Engineer: James W. Cusack
Phone: 315 330-3145

Approved for public release;
distribution unlimited.

This research was supported by the Defense Advanced Research Projects Agency of the Department of Defense and was monitored by James W. Cusack (OCSE), Griffiss AFB NY 13441 under Contract F30602-75-C-0235.

UNCLASSIFIED

SECURITY CLASSIFICATION OF THIS PAGE (When Data Entered)

19 **REPORT DOCUMENTATION PAGE**

READ INSTRUCTIONS BEFORE COMPLETING FORM

18 **1. REPORT NUMBER**
RADC-TR-77-202

2. GOVT ACCESSION NO.

3. RECIPIENT'S CATALOG NUMBER

4. TITLE (and Subtitle)
6 IR ATMOSPHERIC MEASUREMENTS.

5. TYPE OF REPORT & PERIOD COVERED
9 Interim Report.
30 Jun 75 — 28 Feb 76

6. PERFORMING ORG. REPORT NUMBER
N/A

7. AUTHOR(s)
10 H. P. Kent
P. F. Kellen

8. CONTRACT OR GRANT NUMBER(s)
15 F30602-75-C-0235, new ARPA Order-2646

9. PERFORMING ORGANIZATION NAME AND ADDRESS
AVCO Everett Research Laboratory, Inc.
2385 Revere Beach Parkway
Everett MA 02149

10. PROGRAM ELEMENT, PROJECT, TASK AREA & WORK UNIT NUMBERS
62301E
16 26460306 17 03

11. CONTROLLING OFFICE NAME AND ADDRESS
Defense Advanced Research Projects Agency
1400 Wilson Blvd
Arlington VA 22209

12. REPORT DATE
11 June 1977

13. NUMBER OF PAGES
26

14. MONITORING AGENCY NAME & ADDRESS (if different from Controlling Office)
Rome Air Development Center (OCSE)
Griffiss AFB NY 13441
12 31p.

15. SECURITY CLASS. (of this report)
UNCLASSIFIED

15a. DECLASSIFICATION/DOWNGRADING SCHEDULE
N/A

16. DISTRIBUTION STATEMENT (of this Report)
Approved for public release; distribution unlimited.

17. DISTRIBUTION STATEMENT (of the abstract entered in Block 20, if different from Report)
Same

18. SUPPLEMENTARY NOTES
RADC Project Engineer:
James W. Cusack (OCSE)

19. KEY WORDS (Continue on reverse side if necessary and identify by block number)
IR radiometry
Atmospheric extinction
Atmospheric radiance
IR Astronomy
Satellite observations

20. ABSTRACT (Continue on reverse side if necessary and identify by block number)

Atmospheric radiance data obtain enpassant during LWIR observations of satellites may be used to produce a near real-time extinction model for the 20 ~~μm~~ micrometers transmission window. Work is described and some interim results are presented on an experiment intended to characterize atmospheric absorption scaling with wavelength.

Measuring precision of background limited radiometers is improved by long period signal averaging. A facility for accomplishing this is described. (cont'd)

DD FORM 1 JAN 73 1473 EDITION OF 1 NOV 65 IS OBSOLETE

UNCLASSIFIED

SECURITY CLASSIFICATION OF THIS PAGE (When Data Entered)

048 450

JB

UNCLASSIFIED

SECURITY CLASSIFICATION OF THIS PAGE(When Data Entered)

Radiant intensity measurements of asteroids and deep space satellites are presented.

ACCESSION for	
NTIS	White Section ✓
DDC	Buff Section
UNANNOUNCED	
JUSTIFICATION	
BY	
DISTRIBUTION/AVAILABILITY CODES	
Dist.	AVAIL. and/or SPECIAL
A	

UNCLASSIFIED

SECURITY CLASSIFICATION OF THIS PAGE(When Data Entered)

TABLE OF CONTENTS

LIST OF ILLUSTRATIONS

1.0 SCOPE AND BACKGROUND

This report describes work performed and some interim results achieved through February 1976 on the IR Atmospheric Measurements Program.

The program consists of a series of instrumented observations intended: a) to characterize certain optical properties of earth's atmosphere and b) to demonstrate the feasibility of routinely determining the thermal signatures of deep-space earth satellites with an existing sensor at AMOS. Work was begun by AERL in July 1975 in accordance with DARPA contract F30602-75-C-0235 as directed by DARPA's agent: RADC. The program, which was recently modified, is now scheduled to be completed February 1977.

2.0 LONG INTEGRATION SIGNAL PROCESSING - TASK 4.5

Modifications to the signal conditioning and recording facilities of an existing long wave infrared sensor, AMTA, were authorized with the intent of enabling observations of faint deep-space satellites to be made with it routinely. AMTA, like all LWIR point-radiometers used under atmosphere for space observations, is limited in precision by fluctuating emission from both warm atmosphere and optics. At AMOS these two sources produce four to five decades greater flux level, at the detector surface, than typical targets. The line of sight of one or more AMTA detectors is deviated by an oscillating mirror to alternately encompass and exclude the target. AMTA's scan mirror is driven to follow a 45 Hz square-wave which toggles the line of sight 24 arc seconds, an angular distance corresponding to the detector spacing. In the absence of a target, thermal eddies in the atmosphere affect a noise-like detector output which must be integrated to produce a smooth mean value so the target, when present, will obtrude.

Although the spatial distribution of radiant structure in the atmosphere was of intense interest to the IR community in the late 1950's, rather little is available by way of study reports today. Most of this material has been declassified and automatically destroyed. The Weiner spectrum[1] is one enduring description; it predicts the power spectral density of noise, produced by a slot scanning the atmosphere, will vary inversely with the square of spatial frequency. It has been suggested[2] that a corner ought to occur between one and ten cycles per radian, below which the spectrum is uniform. This description suggests that the noise recorded during an observation ought to be highly correlated between detectors which are separated by, at most, 550 μradians. The background is expected to trend monotonically across the array and first order differencing between adjacent 'identical' detector channels should eliminate the influence of atmosphere.

Figure 1 shows how this is accomplished with AMTA. Owing to the toggling motion of the scan mirror and the large scale structure of background granularity, most of the detectors (for this illustration) output 45 Hz signals whose components are in phase between detectors. Detector channel

---

1. University of Michigan report #IRIA 2389-7-X (July 1957).

2. D. Korff, private communication.

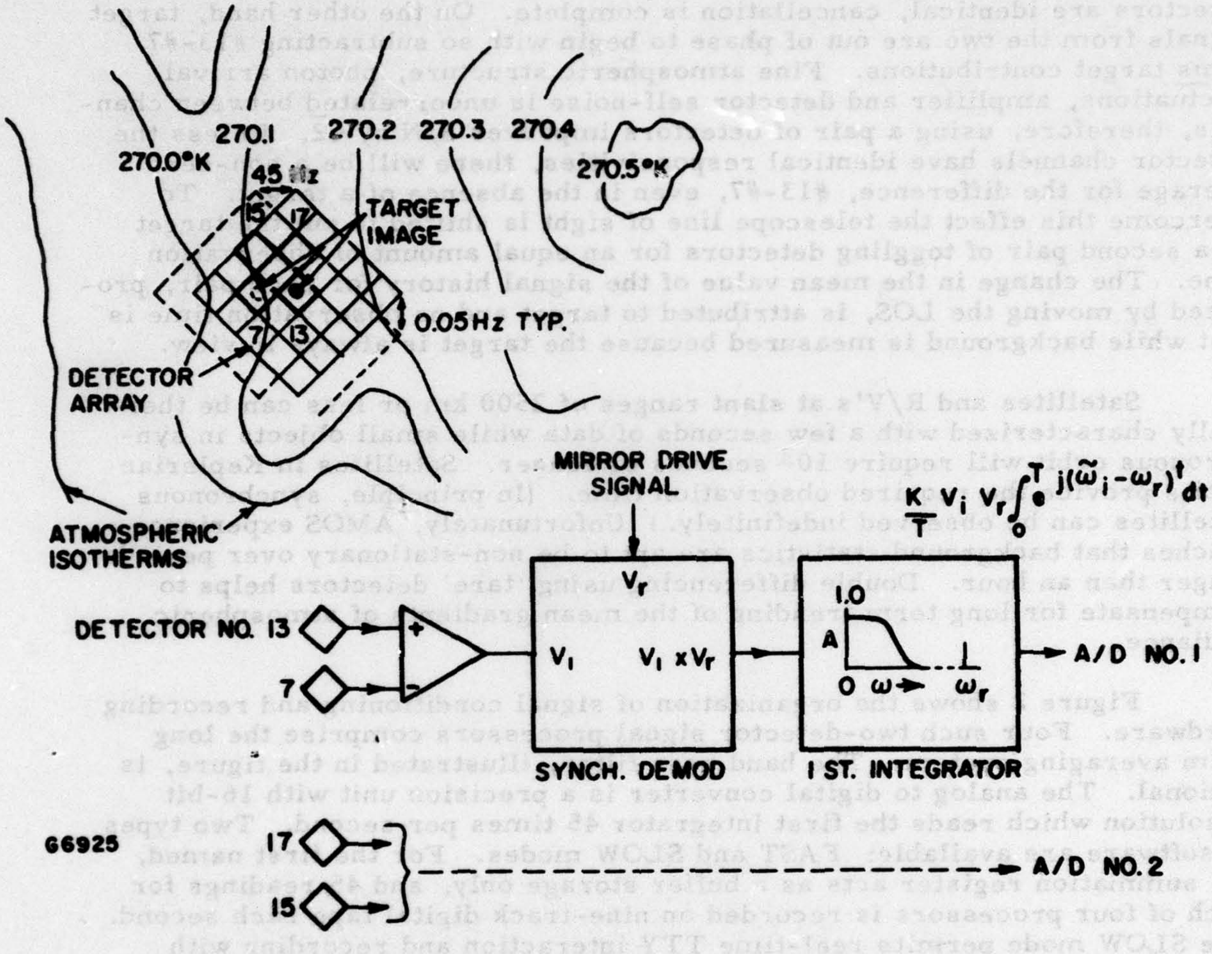

Figure 1 **Retrieving Contrast Features**

#7 is subtracted from channel #13, therefore, background contribution from the two interfere destructively; if the radiant gradient is uniform and the detectors are identical, cancellation is complete. On the other hand, target signals from the two are out of phase to begin with so subtracting #13-#7 sums target contributions. Fine atmospheric structure, photon arrival fluctuations, amplifier and detector self-noise is uncorrelated between channels, therefore, using a pair of detectors improves S/N by $\sqrt{2}$. Unless the detector channels have identical responsivities, there will be a non-zero average for the difference, #13-#7, even in the absence of a target. To overcome this effect the telescope line of sight is shifted to put the target on a second pair of toggling detectors for an equal amount of observation time. The change in the mean value of the signal history for each pair, produced by moving the LOS, is attributed to target and no observation time is lost while background is measured because the target is always in view.

Satellites and R/V's at slant ranges of 2500 km or less can be thermally characterized with a few seconds of data while small objects in synchronous orbit will require 10^3 seconds or longer. Satellites in Keplerian orbits provide the required observation time. (In principle, synchronous satellites can be observed indefinitely.) Unfortunately, AMOS experience teaches that background statistics are apt to be non-stationary over periods longer than an hour. Double differencing using 'tare' detectors helps to compensate for long term trending of the mean gradients of atmospheric radiance.

Figure 2 shows the organization of signal conditioning and recording hardware. Four such two-detector signal processors comprise the long term averaging system. The band pass filter, illustrated in the figure, is optional. The analog to digital converter is a precision unit with 16-bit resolution which reads the first integrator 45 times per second. Two types of software are available: FAST and SLOW modes. For the first named, the summation register acts as a buffer storage only, and 45 readings for each of four processors is recorded on nine-track digital tape each second. The SLOW mode permits real-time TTY interaction and recording with some sacrifice in time resolution: The average of 45 readings is recorded on tape once each second for each processor. The TTY will printout the average of the difference between (pre-selected) pairs of processors once each (preselected) averaging time. The minimum averaging time for this mode is ten seconds; the maximum is 10^4 seconds.

During the course of long observations the background signal, outputted by the first integrator, has changed by as much as a volt per hour (trending) while 10^{-20} w · cm^{-2} target irradiance (a measuring goal) produces 1.7 to 2.0×10^{-5} volts. Seventeen bits are required to encompass this range. The 16-bit converters thus provide a 2×10^{-20} w · cm^{-2} uncertainty per reading. In principle, the mean value of a set of readings may be determined with greater than the encoding resolution by averaging. For example: if two value-adjacent (separated by one least significant bit) digital estimates exactly straddle the actual mean value the least significant bit will be 'lit' for exactly 50% of the sample readings. The average of sixteen readings should

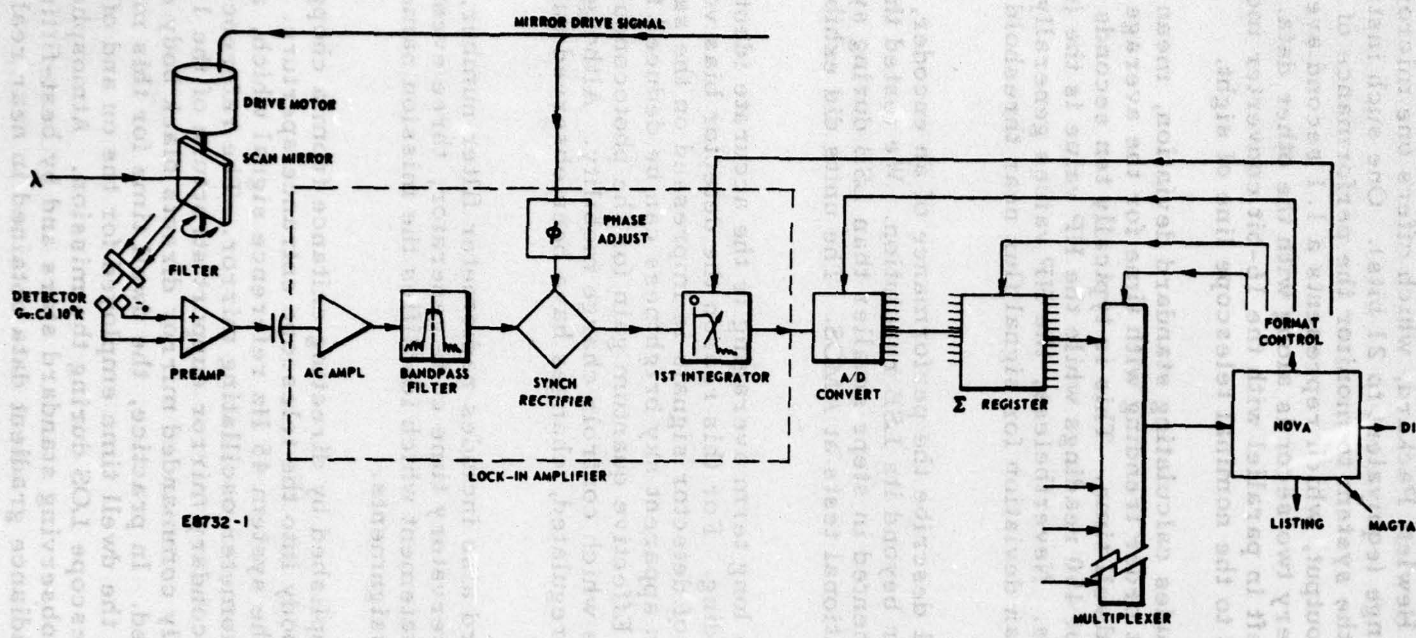

Figure 2 AMTA Signal Processing for Long Integration

yield one additional bit resolution with 90% confidence. Sixteen-bit precision converters are available from two manufacturers. The only available converter with higher resolution is a state-of-the-art oven stabilized digital voltmeter, manufactured by Hewlett Packard, which offers one microvolt resolution over a $\pm$ 1 volt range (equivalent to 21 bits). One such instrument was incorporated into the system to monitor the performance of the other converters. Its BCD output, which represents a 1.1 second averaged reading is recorded once every two seconds along with the other data. The HP voltmeter is generally left in parallel with the 16-bit converter monitoring the detector pair closest to the nominal telescope line of sight.

Data processing includes calculating standard deviation, mean value and least-squares fit to first order trending with time for the average values obtained per telescope LOS dwell time. This is typically ten seconds so the 16-bit value is the average of 450 readings while the HP value is the (second) average of only five readings. Nevertheless, the HP values generally have 10% smaller normalized mean deviation for signal flux near threshold for five minute observations.

No manufacturer will describe the performance of an encoder, a voltmeter, or A/D converter beyond its LSB resolution. We tested the 16-bit units with signals incremented in steps smaller than LSB during system tests and again during operational tests at AMOS. The units did exhibit the ability to interpolate.

The key limitation to long term averaging is the accurate identification of all sources of trending. For this reason the detector bias voltage bus and the 'absolute' value of detector signals is impressed on the same nine-track tape. Changes in apparent sky brightness can be deduced from the absolute value history. Effective quantum gain for the photoconductors is a function of detector bias which controls charge mobility. Although the bias bus is reasonably well regulated, changes have been observed during long integration missions.

The nine-track record also includes radiometer filter number, Universal time from the observatory time code generator, three event flags and a typed-in initializing statement which identifies the mission name, date and detector channel assignments.

Calibration is accomplished by directing exitance from a chopper modulated reference black body into the telescope entrance aperture. The chopper is phase locked to the system 45 Hz reference signal which, at other times, drives the radiometer oscillating mirror. The reference source is mounted on the secondary mirror support structure of the 1.2 meter telescope. A remotely commanded mirror directs black body energy into the telescope as required. In practice, the dwell time for this mirror is adjusted to correspond to the dwell time employed for the on and off-axis detector channels by the telescope LOS during the mission. Atmospheric extinction is determined by observing standard stars and by best-fitting an absorptance model to sky radiance gradient data obtained in near real time.

2.1 RESULTS

LWIR flux from certain stars, two asteroids and a number of deep space satellites were measured with the new system in January 1976. Some results are presented here:

Long Integration

ADC #	Date	Time	Name	Range	Elev.	Filter	Intensity $w \cdot ster^{-1}$
6356	24 January	10:40	Moly 1-23	37500	39.5^{o}	5	530 ± 120
7625	23 January	08:15	COS #706	40440	52.5^{o}	5	360 ± 160
6356	22 January	09:30	Moly 1-23	29900	39.8^{o}	5	730 ± 250
83564	22 January	09:59	DSP	39223	23.0^{o}	5	450 ± 360
83564	28 January	08:10	DSP	39270	23.1^{o}	5	640 ± 136
83564	28 January	08:30	DSP	39269	23.1^{o}	6	<410

The intensities recorded were obtained with ≤ 600 seconds integration. DSP is a U.S. satellite in synchronous orbit while the others are USSR objects in highly elliptical half-day orbits. The 20 μm (filter #6) bounding value listed for DSP represents the standard deviation about the background. The signal history showed no repeatable increase when the FOV encompassed the target during the observation. The results of an earlier observation of Molniya 1-19 is shown in Figure 3.

Infrared observations were made of the following astronomical objects:

Star Name	AMTA Filter #	Objectives
β And	2, 5, 6	Calibration and extinction determination
α Tan	2, 5, 6	" " "
R Leo	2, 5, 6	" " "
R Hya	2, 5, 6	" " "
MNL Cyg	5, 6	" " "
ι Per	5, 6	Long average observation
δ Tan	5, 6	" " "
γ Hya	5	" " "

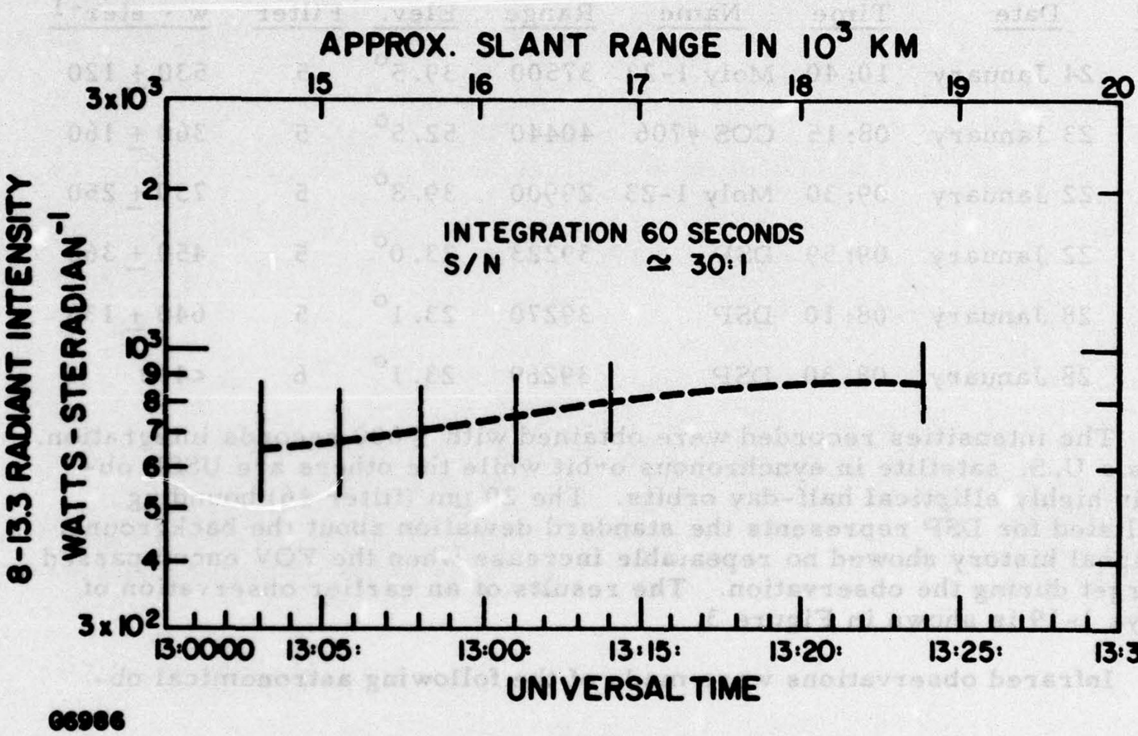

Figure 3 Molniya 1-19 Thermal Signature

Star Name	AMTA Filter #	Objectives
β Her	5	Long average observation
τ Pup	5	" " "

Asteroids	AMTA Filter #	Objectives
Ceres	2, 5, 6	Temperature measurement test
Juno	5, 6	" " "
Vesta	2, 5, 6	" " "

The first five are bright, familiar, infrared stars which, with the exception of β And, are used for AMTA calibration in support of observations generally not requiring integration beyond one second. The signatures obtained for α Tau, MNL Cyg, R Leo and R Hya were repeatable night after night within $\pm$ 2% and correspond to catalog values(3), (4) within $\pm$ 9% for filters #5 and #2. Correspondency at 20 μm (filter #6) was considerably poorer: $\pm$58% or 0.5 stellar magnitudes. This is probably due to incorrect atmospheric extinction assumptions both at AMOS and at U. Arizona. Considerably fewer m_Q observations are published than either m_N or m_M. AMOS brightness results for β And compare well with recent observations by F. J. Low and G. Rieke (5):

	m_M	m_N	m_Q	T_{eff}(N/Q)	T_{eff}(M/N)
AMOS	-1.87	-2.13	-2.41	1300°K	2740°K
Ref 7	-1.97	-2.05	-2.20	2130°K	5500°K
λ_{eff}	5 μm	10.6 μ	21 μm		

3. Heath, J., AMOS Star Library, Lockheed Missiles and Space Company, Inc. (April 1974).
4. F. J. Low, Sky Survey, Semi-Annual Technical Report, AFCRL #70-0179, Univ. of Arizona (15 March 1970).
5. N. Carleton (editor), Methods of Experimental Physics, Vol. 12, Astrophysics, p. 453, Academic Press, N.Y. (1974).

The temperatures listed are calculated by fitting the indicated two color spectral irradiances to a black body. β And is listed[6] as spectral type MO III star, which suggests[7] a visual color temperature of 3200°K, and as a suspected variable, [6] which might easily account for the different apparent temperatures observed.

The next five stars listed in the observation table are much fainter. These were selected to demonstrate that familiar visual stars which are known to be stable and free of spectral trauma (principally class V, sun-like stars) should have predictable signatures in the LWIR. If this proves to be true, such stars provide useful calibration standards now that long integration has produced the required sensitivity. Figure 4 relates visual brightness to 8 to 13 μm irradiance for normal stars by spectral type. By way of example, note that a sun-like star (5800°K) with brightness $m_V = 3.5$ is expected to produce 3:1 S/N at 10 μm with ten second integration. Excepting δ Tau, none of those observed are listed in our rather extensive LWIR star catalogs. Reference 6, which describes observations made before March 1970, reports $m_N = +2.55$ for this star. Our own measurements indicate $m_N = +1.50$ and these results repeat within 0.3 stellar magnitudes.

Of the three asteroids observed two, Ceres and Juno, yield temperature and diameter estimates while 'Vesta' exceeded background only for 5 μm (filter #2). I suspect we were actually looking at an $m_V = +8.9$, KO star (GC 818). The apparent surface temperature of the asteroids Ceres and Juno was measured using the newly installed system. Multicolor data from 20 and 22 January observations were also used to determine size and surface albedo for these objects. The newly developed atmospheric extinction models were used for filter #6 data.

	m_{ph} [10]	radius, km		Range, km[10]	Temp °K	a_S
		AMOS	Allen[9]			
Ceres	+7.7	409±34	380	3.049×10^8	235±7.4°K	0.86
Juno	+9.6	155±33	100	2.693×10^8	215±18.3°K	0.51

It is assumed that these objects radiate as grey bodies between 8 and 22 μm with emissivity something like earth's moon, i.e.: $\epsilon_{TH} \simeq 0.89$.

6. Hoffleit, D., Catalog of Bright Stars, 3rd Ed. Yale University Observ. (1964).
7. C.W. Allen, Astrophysical Quantities, 3rd Ed. p. 206, Univ. of London, Athlone Press (1973).
8. American Ephemeris and Nautical Almanac for 1976, U.S. GPO.

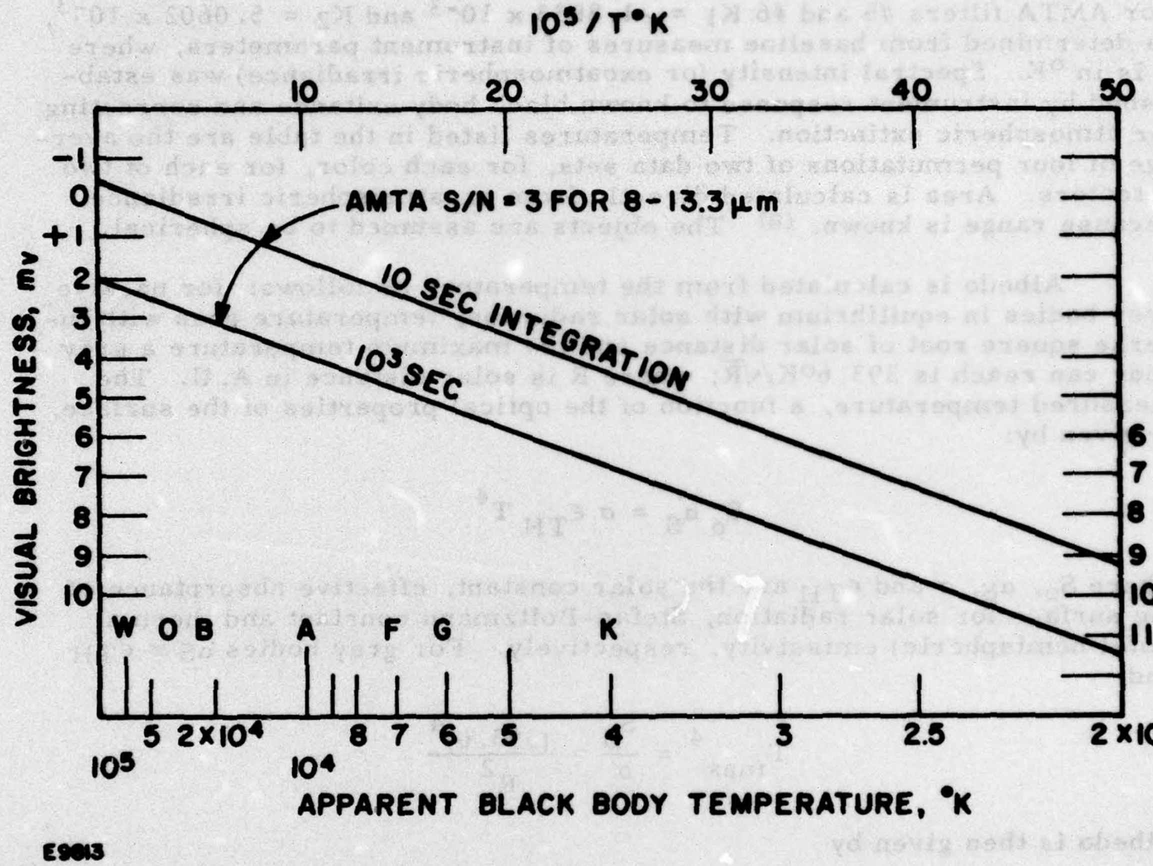

Figure 4 Normal Stars as LWIR Standards

In the regime where $e^{C_2/\lambda T} \gg 1$ spectral intensity of thermal radiators is exponentially proportional to inverse temperature, and obversely, temperature is given by

$$T = \left[K_1 \ln \frac{I_{\lambda 1}}{I_{\lambda 2}} + K_2\right]^{-1}, \; I_{\lambda 1} \text{ and } I_{\lambda 2} \text{ is intensity at } \lambda 1 \text{ and } \lambda 2.$$

For AMTA filters #5 and #6 $K_1 = -1.8833 \times 10^{-3}$ and $K_2 = 5.0602 \times 10^{-3}$, as determined from baseline measures of instrument parameters, where T is in ^{o}K. Spectral intensity (or exoatmospheric irradiance) was established by instrument response to known black body exitance and correcting for atmospheric extinction. Temperatures listed in the table are the average of four permutations of two data sets, for each color, for each of two detectors. Area is calculated directly from exoatmospheric irradiance because range is known. (8) The objects are assumed to be spherical.

Albedo is calculated from the temperature as follows: for passive grey bodies in equilibrium with solar radiation, temperature goes with inverse square root of solar distance and the maximum temperature a grey body can reach is $393.6^{o}K/\sqrt{R}$; where R is solar distance in A. U. The measured temperature, a function of the optical properties of the surface, is given by:

$$S_o \, \alpha_S = \sigma \, \epsilon_{TH} \, T^4$$

where S_o, α_S, σ and ϵ_{TH} are the solar constant, effective absorptance of the surface for solar radiation, Stefan-Boltzmann constant and thermal (total hemispheric) emissivity, respectively. For grey bodies $\alpha_S \equiv \epsilon_{TH}$ and

$$T_{max}{}^4 = \frac{S_o}{\sigma} = \frac{(393.6)^4}{R^2}$$

Albedo is then given by

$$1 - \alpha_S = 1 - \frac{R^2 T^4}{(393.6)^4} \, \epsilon_{TH}$$

Observation of Ceres, Juno and stars for calibrating the sensor yielded data for calculating NEFD; some results are given here:

NEFD, Filter #5	Integration Time			
Det. #	1 sec	120 sec	360 sec	600 sec
13	18Z	4.9Z	1.1Z	0.77Z
25	13Z	3.2Z	2.5Z	0.76Z

NEFD, Filter #6 Integration Time				
Det. #	1 sec	120 sec	360 sec	600 sec
25	26Z	6. 2Z	4. 3Z	
13	21Z	3. 7Z		2. 4Z

The noise equivalent flux density is determined from the standard deviation about the mean for stellar signals. Popular practice for reporting sensitivity entails dividing measured s. d. by the square-root of the number of readings; while this yields a more satisfying result, it is mathematically correct only for stationary random processes where the individual readings are truly independent. With long term trends produced by small local weather condition changes one cannot be certain the statistical properties of the background remain stationary. Note that these results apply to single detectors: #13 and #25, not combinations of two adjacent detectors discussed earlier. The double differencing capability had not been tested during the performance period covered by this report.

3.0 ATMOSPHERIC EXTINCTION SCALING - TASK 4.1

Thermal observations of foreign satellites can yield important mission clues. The effective surface temperature of operational satellites may be determined by making multi-color measurements of thermal exitance. When such observations are made from beneath atmosphere extinction correction uncertainties at long wavelengths can seriously limit the validity of conclusions. The principal source of uncertainty is the amount of H_2O, which strongly affects absorption in the Q-window (16-23 μm) region, along the line of sight. On mountain tops, where abrupt weather modifications are common, water vapor content changes so rapidly that extinction, determined by observing stars, may not be applicable to a satellite measurement made an hour later. During the course of such observations we have recorded a monotonic increase, with increasing zenity distance, in LWIR radiometer output when the instrument is looking at clear sky. This signal at 20 μm is principally due to thermal emission from atmospheric water vapor.* By measuring radiance gradient an absorption model may be calculated. Moreover, if the radiometer is arranged to provide an absolute measure of background radiance, extinction may be deduced for a satellite mission even when there is no orderly relation between absorptance and zenith distance.

To prove this concept facilities for measuring and recording mean detector resistance for ten detector channels were incorporated into the AMTA system. This facility shares a tape recorder, rack space and a minicomputer with the long period averaging system described earlier in this report. Resistance (actually d.c. detector output) is monitored, digitized, multiplexed, averaged and recorded on nine-track digital tape along with the contrast data from astronomical and satellite observations without interfering with or degrading AMTA performance in any way. The hardware was installed at AMOS in December 1975 and became operational in January. Figure 6 is a system block diagram of the extinction measuring add-on for AMTA.

The d.c. output of each of ten detectors is digitized with 12-bits per ten volts resolution, eight times each minor scan cycle. The four readings for each of the two scan mirror positions are averaged and recorded separately. This produces ninety recorded readings, each second, for each detector. These numbers are retrieved from tape and averaged to any desired degree of smoothness along with the mission data. An eleventh 12-bit A/D converter monitors detector bias which is also recorded on tape ninety times per second.

---

*See Figure 5.

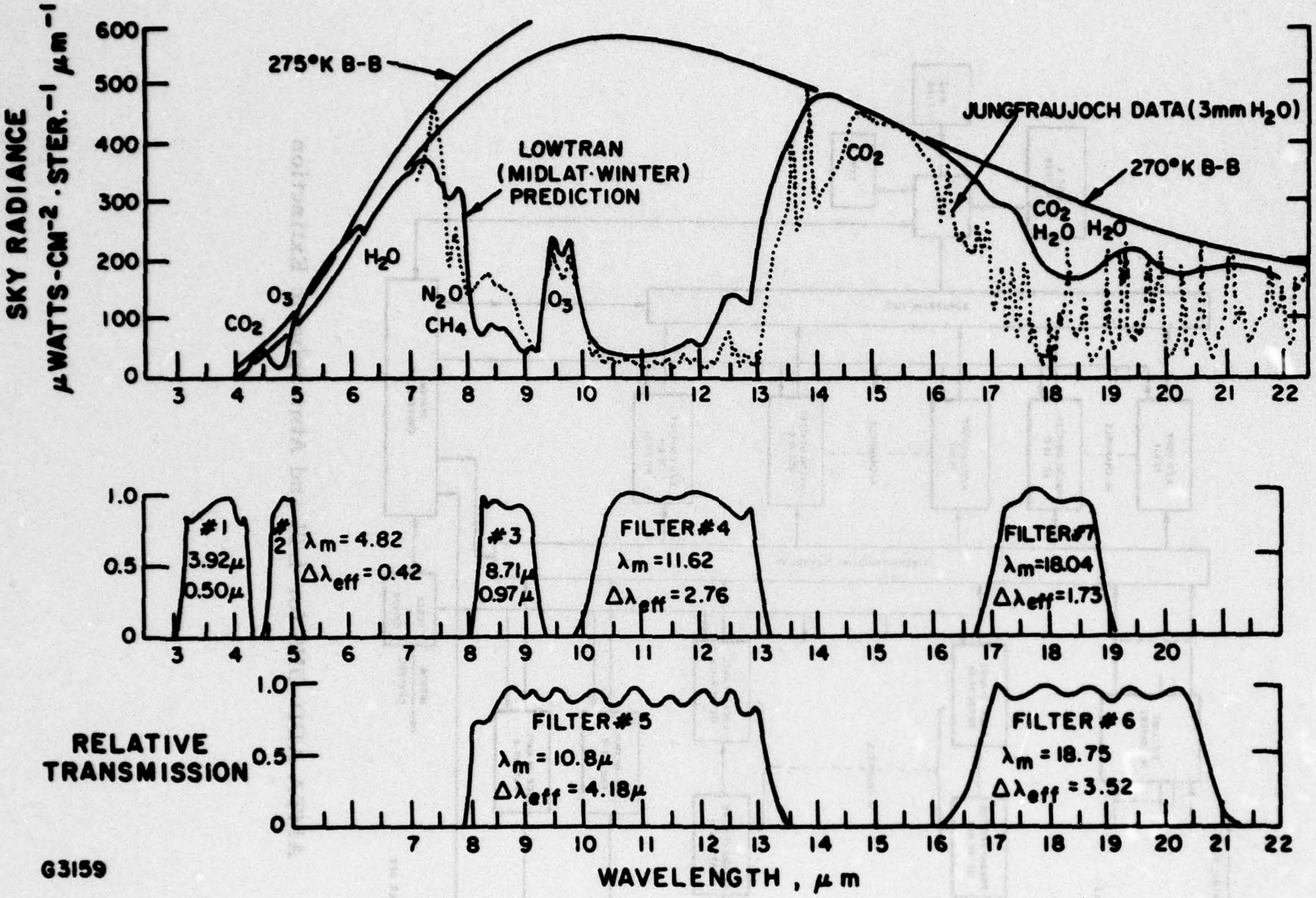

Figure 5 Sky Radiance Measurement

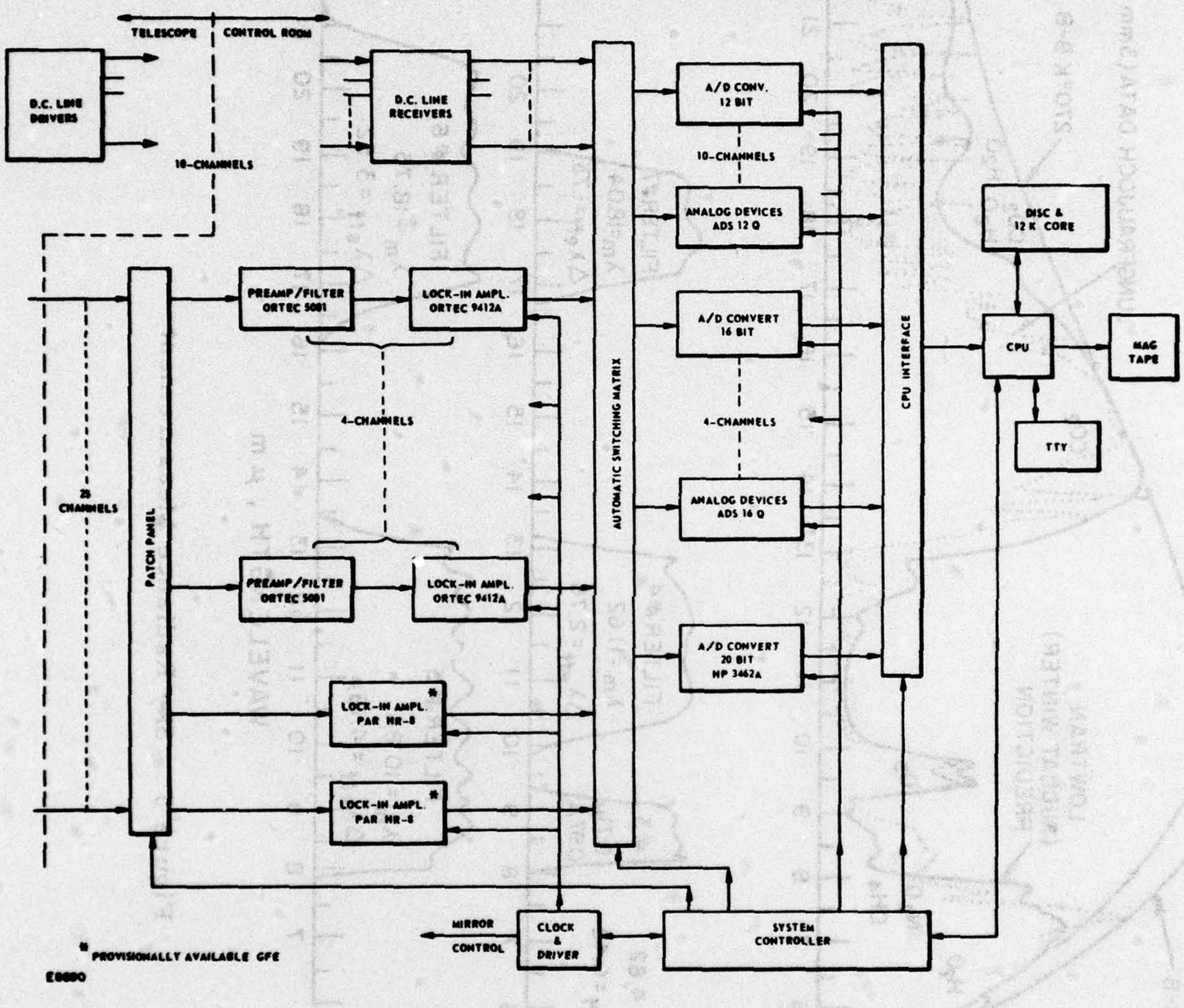

Figure 6 AMTA ADD-ONS for LTI and Atmospheric Extinction

Detector voltage is related to absolute radiance by means of the same black body reference source used to interpret mission data. To unwind instrument bias and off-set due to emission of the optics the sensor filter wheel is rotated to block all detectors with an opaque port refrigerated, like the filters themselves, to $\simeq 40°K$. The detector array lies at the bottom of a cylindrical low reflectance light shield and is maintained at 11° to 14°K. The array semiconductors will not respond to photons less energetic than 22 μm; the blocked light shield thus establishes the 'zero photon' detector resistances. Next, the blocking port is replaced with the interference filter(s) to be used during the mission; (the AMTA filter wheel is remotely commanded and its disposition is automatically recorded on the data tape once each second) and the telescope dust-covers are closed. The resulting detector outputs represents response to the optical train exitance with assumed unity emissivity. The calculated emissivity for all cascaded optical surfaces which are not refrigerated is $\epsilon = 0.205$. This value is applied to the difference between the dust cover reading and the blocked detector reading to establish what fraction of the output, recorded during the measurement, to attribute to warm instrument optics.

In January 1976 tests were conducted with the newly installed hardware to confirm the validity of relating atmospheric brightness to transmission. Measurement procedures were described in MIOP 015 (Mission Instruction and Operational Plan) distributed at AMOS. The data taken in January did produce a plausible zenith distance related expression for atmospheric extinction but sufficient 'standard star' observations to fully validate the model were not undertaken, due to press of other work. The model at 20 μm (filter #6) assumes, since most of the water is in the first 2 km above AMOS, that a temperature scaled 1.4 km above altitude can be assigned to the dominant radiating constituent and that the output produced by looking just above 0° elevation is representative of total absorption ($\epsilon = 1.0$).

The data tapes were reduced in Everett where software for computing extinction from spectral radiance data was completed and exercised with "sky scan" radiance data obtained from AMOS as a result of January activities there.

The apparent spectral radiance of the atmosphere is attributed to its effective temperature and emissivity. A radiance gradient measurement will yield emissivity and transmission since $1 - \epsilon(\lambda) = \tau(\lambda)$. Transmission as function of elevation angle is given by

$$\tau(\lambda) = \exp \frac{-\alpha(\lambda)}{\left(\frac{P_o}{P_h} \sin El\right)^{\beta(\lambda)}} \quad \text{for uniform exponential atmosphere} \qquad (1)$$

above $\simeq 10°$ elevation (4 air masses at AMOS). P_h, P_o are atmospheric pressure at the altitude of the observer and sea level respectively; and $\beta(\lambda)$ is a number, ≤ 1.0, depending upon the concentration profile of the absorbing medium and whether the line absorbers are saturated. In the visible, where extinction is attributed primarily to scattering and the medium is tenuous for broad spectral intervals, $\beta(\text{vis}) = 1.0$. In the LWIR where molecular absorption dominates, and the line centers are apt to be saturated, theory predicts $\beta(\lambda) \geq 0.5$. The radiance data obtained in January seems to bear this out at 19 μm but not at 10 μm.

The data recorded on magnetic tape 22 January 1976 consists of a time-tagged history of d.c. voltage outputted by five detector channels while the telescope stepped in elevation from $+4^o$ to zenith in accordance with a prearranged schedule. Since detector channel output change is linearly proportional to radiance change:

$$E(El) = E_o\,[1 - \tau(\lambda)],$$

$$E(El) = E_o\left[1 - \exp\frac{-\alpha(\lambda)}{\left(\frac{P_o}{P_h}\sin Ei\right)^{\beta(\lambda)}}\right] \text{ and ultimately} \qquad (2)$$

$$\ln\ln\frac{E_o}{E_o - E(El)} = \ln\alpha(\lambda) - \beta(\lambda)\ln\left(\frac{P_o}{P_h}\sin El\right);$$

which can be fitted by least squares to the data* to yield $\alpha(\lambda)$ and $\beta(\lambda)$. E_o is detector response to a black radiator at the effective temperature of the atmosphere; for 20 μm this is essentially the voltage for zero elevation. Sky scans were made for filters 2, 5, 6 and 7.

Filter #5 (λ_m = 10.9 μm, $\Delta\lambda$ = 4.1 μm) and #6 (λ_m = 18.9 μm, $\Delta\lambda$ = 3.3 μm) data was reduced with the new program to yield the following results:

	$\alpha(\lambda) \pm \sigma$	$\beta(\lambda) \pm \sigma$
Filter #5	0.200 ± .006	0.372 ± .008
Filter #6	1.109 ± .011	0.610 ± .028

	Zenith	45^o Elev.	20^o Elev.
Filter #5, τ(10.9 μm)	0.84 ± .004	0.82 ± .004	0.77 ± .004
Filter #6, τ(18.9 μm)	0.41 ± .004	0.33 ± .004	0.18 ± .008
Air Masses	0.704	0.996	2.058

*See Figure 7 for samples of raw data; detector voltage is plotted against equivalent sea level air masses for filters 2, 5, 6 and 7.

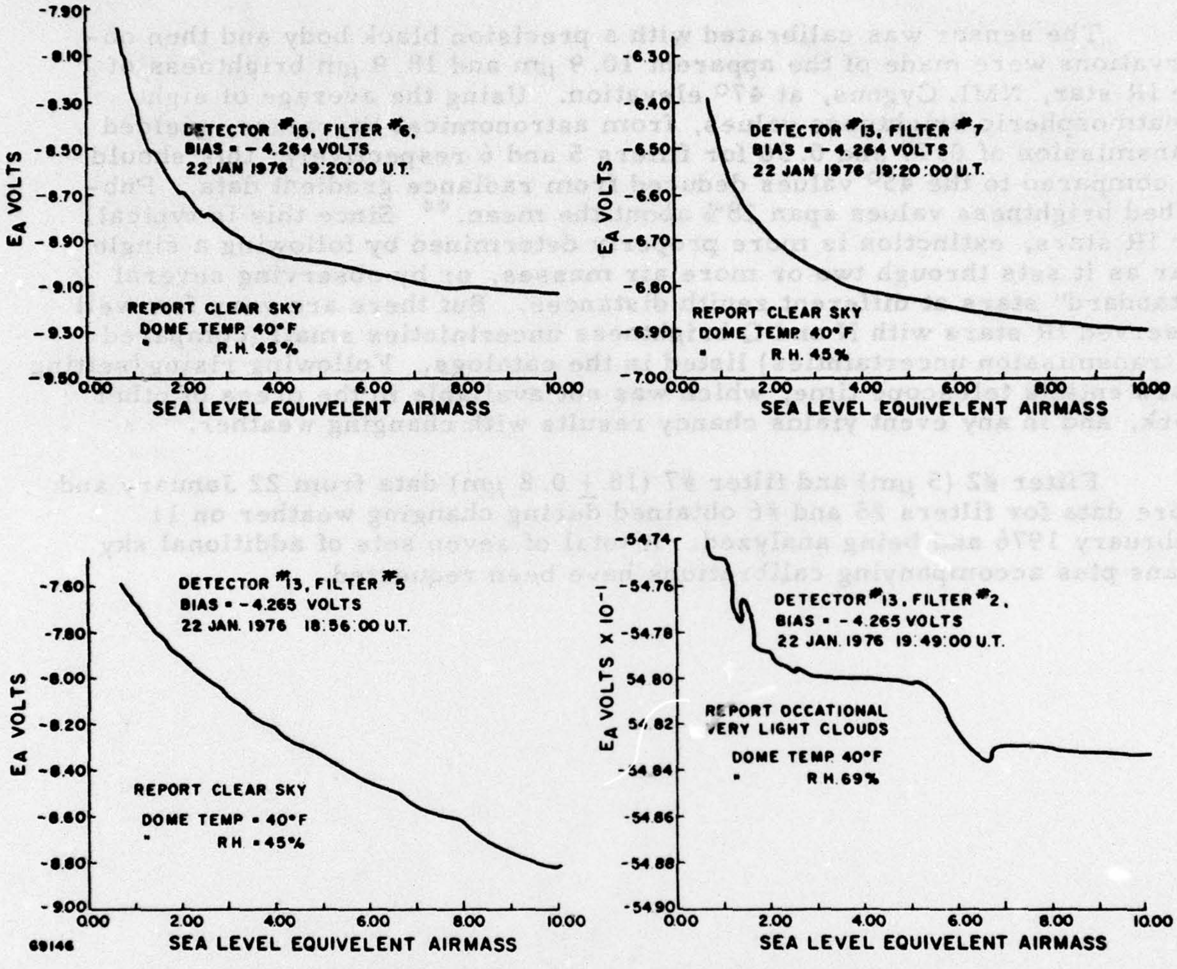

Figure 7 Air Masses Related to Detector Output

The values and scatter for $\alpha(\lambda)$ and $\beta(\lambda)$ are the averages for five detectors; Eq. (1) was used to compute transmission.

The sensor was calibrated with a precision black body and then observations were made of the apparent 10.9 μm and 18.9 μm brightness of the IR star, NML Cygnus, at 47° elevation. Using the average of eight exoatmospheric brightness values, from astronomical literature, yielded transmission of 0.77 and 0.30 for filters 5 and 6 respectively; this should be compared to the 45° values deduced from radiance gradient data. Published brightness values span 28% about the mean.** Since this is typical for IR stars, extinction is more properly determined by following a single star as it sets through two or more air masses, or by observing several "standard" stars at different zenith distances. But there are very few well observed IR stars with N and Q brightness uncertainties small (compared to transmission uncertainties) listed in the catalogs. Following rising/setting stars entails telescope time, which was not available in the press of other work, and in any event yields chancy results with changing weather.

Filter #2 (5 μm) and filter #7 (18 $\pm$ 0.8 μm) data from 22 January and more data for filters #5 and #6 obtained during changing weather on 11 February 1976 and being analyzed. A total of seven sets of additional sky scans plus accompanying calibrations have been requested.

** Note that the ratio of $\tau(18.9)/\tau(10.9)$ reduced from radiance measures and from star data agree very closely: 0.39 and 0.40 respectively; the apparent temperature of NML Cyg is better known than its brightness.

4.0 MEASURING PRECISION CONSTRAINTS

To improve immunity to the AMOS EMI environment, some long term drift problems attributed to cabinet temperature changes and common mode response problems, hardware modifications described during the 19 February briefing are being implemented. Fabrication is 20% complete and an additional twenty man days of labor should suffice to complete this work.

The sky scan data produced verification of the long reported belief that radiant structure in the atmosphere limits the sensitivity of a fast-slewing radiometer. Wind driven eddies are observed at AMOS even when tracking stars; F. J. Low[5] refers to 'sky noise' which is probably the same thing. The sky scan measuring procedure in January involved moving the telescope up from the horizon to zenith in an orderly series of step-stare operations. Detector resistance (d. c. voltage) was recorded for five channels in order to chart the relation between apparent brightness and zenith distance as explained earlier. The highly amplified a. c. outputs were recorded too. This was done to provide data relating NEFD to zenith distance, a sort of no-effort aside to the primary measurement. It turned out that deviation about the mean background was consistently higher for 'step' than for 'stare'. Standard deviation of the recorded bakcground was converted to equivalent entrance aperture flux by relating to the output voltage change produced by the black body reference source. The results are plotted in Figure 8. The dotted trace is a least-squares fit to the 'stepping' data; the solid curve, which ties the 'stare' points together, is calculated for 'still-air' sky and shifted upward a factor of six. Note that above 40^{o} elevation moving the telescope produces a factor of two more 'uncertainty', but conditions wherein motion makes no difference do exist here while, at lower elevation, motion consistently degraded measuring precision. On rare occasions measurements near zenith with a fixed telescope have yielded 2.5 x Z NEFD. The results shown with slewing help to explain why data from satellites in low orbit and data obtained at low elevation is so unexpectedly 'ragged'. Experiments for characterizing the spatial frequency density distribution of radiant atmospheric structure (Weiner spectrum measurements) have been discussed.

As self-scanning (CCD, CID, etc) focal planes develop and extremely populous arrays become practical, real time clutter cancellation becomes a distinct possibility. Dave Fried has suggested that, if detector spacing is at least twice as fine as the finest significant atmospheric clutter, the clutter in the track direction is completely defined and its interference with a stationary target becomes surmountable. Weiner spectrum information is needed to define the required pixel and frame rate scaling.

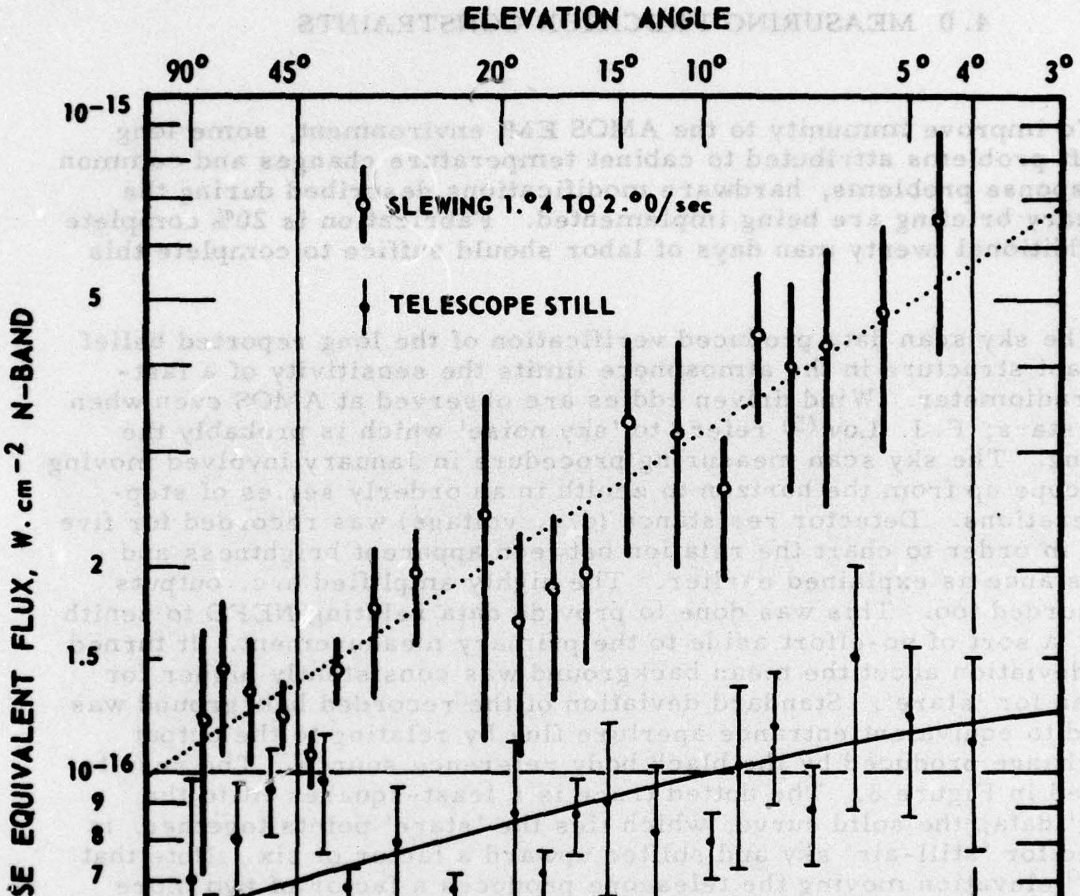

Figure 8 Sensitivity with Slewing

REFERENCES

1. University of Michigan report #IRIA 2389-7-X (July 1957).
2. D. Korff, private communication.
3. Heath, J., AMOS Star Library, Lockheed Missiles and Space Company, Inc. (April 1974).
4. F. J. Low, Sky Survey, Semi-Annual Technical Report, AFCRL #70-0179, Univ. of Arizona (15 March 1970).
5. N. Carleton (editor), Methods of Experimental Physics, Vol. 12, Astrophysics, p. 453, Academic Press, N. Y. (1974).
6. Hoffleit, D., Catalog of Bright Stars, 3rd Ed. Yale University Observ. (1964).
7. C. W. Allen, Astrophysical Quantities, 3rd Ed. p. 206, Univ. of London, Athlone Press (1973).
8. American Ephemeris and Nautical Almanac for 1976, U. S. GPO.